

# Tactile Sensing for Mobile Manipulation

Sachin Chitta<sup>1</sup>Jürgen Sturm<sup>2</sup>Matthew Piccoli<sup>3</sup>Wolfram Burgard<sup>2</sup>

**Abstract**—Tactile information is valuable in determining properties of objects that are inaccessible from visual perception. In this work, we present a tactile perception strategy that allows a mobile robot with tactile sensors in its gripper to measure a generic set of tactile features while manipulating an object. We propose a switching velocity-force controller that grasps an object safely and reveals at the same time its deformation properties. By gently rolling the object, the robot can extract additional information about the contents of the object. As an application, we show that a robot can use these features to distinguish the internal state of bottles and cans — purely from tactile sensing — from a small training set. The robot can distinguish open from closed bottles and cans, and full ones from empty ones. We also show how the high-frequency component in tactile information can be used to detect movement inside a container, e.g., in order to detect the presence of liquid. To prove that this is a hard recognition problem, we also conducted a comparative study with 17 human test subjects. The recognition rates of the human subjects were comparable to that of the robot.

## I. INTRODUCTION

Humans have a remarkable sense of touch that enables them to explore their environment in the finest detail [1], [2]. Tactile feedback provides subtle cues about the environment that cannot be obtained from any other perceptual sensors. Tactile feedback allows us to localize objects in our hand, determine their rigidity as well as other material properties, and even their identity. Consider, for example, the task of choosing fruit: the response of the fruit quickly lets us figure out whether it is ripe. Another example is to clean a table full of bottles: in order not to spill anything, knowing which bottles contain liquid means knowing which ones need to be manipulated with care.

Human skin contains a variety of touch-sensitive cells, that signal the deformation of the skin to the brain. The human hand is equipped with four different types of tactile afferents, that respond to tactile stimuli at different frequencies and temporal scales [2]. Neuro-physiological evidence exists that suggests the specific form of the fingers including the fingernail enables the perception of oriented fingertip forces [3].

Tactile sensors provide robots with additional means of sensing the objects they are manipulating. On the hardware side, tactile sensors range from simple contact switches that provide binary information about whether the robot is in contact with the environment to more complex arrays of sensors that provide pressure sensing at a resolution comparable to



Fig. 1. **Top left:** A mobile manipulation robot grasping a bottle estimates both object class as well as the state of the grasped object from its tactile appearance. **Top right:** Comparative study on tactile performance with human test subjects. **Bottom:** The robot estimates whether liquid is in the bottle by rolling it. The robot extracts peaks of high-frequency using its touch-sensitive fingertips.

human fingertips [4]–[9]. Force-torque sensors mounted on the wrist of a robot are also often used to provide tactile information about the environment, but are in general less accurate than tactile sensing in the fingertips.

Various approaches have been proposed on tactile information processing, but it has largely remained unclear what information a robot can deduce reliably from tactile data and how it can use this information to support object manipulation. Therefore, our focus in this work has been to develop a set of generic tactile features that can be easily extracted from most tactile sensors, and that facilitate the usage of tactile information. More specifically, we present a set of six generic tactile features that describe the deformation properties of objects being manipulated, like the object size, the compression ratio and compression velocity. These features can then be used by standard machine learning techniques to learn a classifier for recognizing different internal states. In our concrete evaluation scenario, we apply our approach to the problem of discriminating between various types of liquid containers (water bottles, soda cans, or fruit juice bottles) and their respective internal states (full, empty, open, or closed). A robot can use this information both for low-level motor control

<sup>1</sup> Sachin Chitta is with Willow Garage Inc., Menlo Park, CA 94025, USA [sachinc@willowgarage.com](mailto:sachinc@willowgarage.com)

<sup>2</sup> Jürgen Sturm and Wolfram Burgard are with the Autonomous Intelligent Systems Lab, Computer Science Department, University of Freiburg, Germany [sturm@informatik.uni-freiburg.de](mailto:sturm@informatik.uni-freiburg.de)

<sup>3</sup> Matthew Piccoli is with the Grasp Laboratory, University of Pennsylvania, Philadelphia, PA 19104 [piccolli@me.upenn.edu](mailto:piccolli@me.upenn.edu)

and higher-level motion planning algorithms with the aim to make object manipulation more robust. For example, the robot can select an appropriate gripping force, manipulation speed, or impose other constraints, in order to neither spill liquid nor crush the bottle. We compare the results from these experiments to human-study experiments, where human subjects were asked to discriminate among the same set of objects. The results of this study inspired us to consider an additional tactile feature based on high-frequency components in the tactile signals. In further experiments, we found that this feature is particularly well suited for indicating the presence of liquid in containers while the container is actuated.

### A. Related Work

Several studies have shown that humans are very good at modulating the applied grasp force in relation to the expected load force [1], [10]. Even during dynamic motions such as walking or running, humans always apply the minimum force required to hold an object safely. These coordinative constraints simplify the control by reducing several degrees-of-freedom during the manipulation tasks. Tactile perception hereby plays an essential role: In experiments with humans, it was shown that the test subjects exerted much more gripping force than actually was needed when their fingertips are anesthetized, even if visual feedback was available [11]. Recently, McMahan et al. [12] have shown that high-bandwidth haptic playback significantly improves the perceived realism of a master-slave tele-operation system.

Dahiya et al. [4] provide both a good introduction on tactile sensing in humans, and a detailed discussion of approaches on the development of tactile sensors for robots. Recent developments in sensor hardware include the work of Weiss et al. [6] on resistive sensor cells, Ohumura et al [7] on a flexible sensor skin, Ueda et al. [8] on vision-based tactile finger tip sensors.

Bierbaum et al. [13] presented recently an approach for tactile exploration of objects using a five-fingered hand based on potential fields. Schneider et al. [14] used tactile sensing for object recognition. They applied a variant of the bag-of-features approach to the tactile images, and showed that the robot could recognize a large set of different objects. The authors also presented an exploration strategy that optimizes the number of grasps based on the expected information gain. Gorges et al. [15] recognized different objects based on tactile and kinesthetic sensors using self-organizing maps (SOMs). In their experiments, they found that additional passive degrees of freedom between the robotic fingers and the tactile sensor array improved the recognition rates significantly. Takamuku et al. [16] use an anthropomorphic hand for recognizing objects. In their experiments Takamuku et al. found that the recognition rate improves significantly after repeatedly opening and closed the hand around the object, until the object converges into a discriminative position.

By using acoustic sensors only, Griffith et al. [17] used unsupervised clustering for discriminating container objects from non-containers, by the sound objects make by falling inside or on top of other objects. However, recording sound without

background noises is difficult with a moving manipulator, and in crowded environments. In contrast to that, tactile sensors directly measure the interaction of the object with the robotic gripper.

Prior work [18], [19] exists on estimating the friction coefficients such that slippage and crushing are avoided. Maeno [18] gives a good overview over existing techniques and describes how their system estimates these values from the tangential forces while pushing a tactile sensor into a surface. Frank et al. [20] use a force-torque sensor in combination with a depth camera for estimating the deformation coefficients. Saal et al. [21] estimate the dynamic parameters of objects using tactile sensors. The robot optimizes the shaking behavior to speed up the convergence.

Our approach differs from previous approaches as our aim of estimation is different. The goal of our approach is to extract a generic set of features from the tactile data that a robot can use to estimate the internal state of grasped objects. Although we have tested our features using the two-fingered gripper on the PR2 robot (Figure 3), we believe that the features can easily be adapted for use with other types of grippers. Another contribution of this paper is that we provide a human study in which we asked human subjects to perform the same recognition tasks as the robot. The results of this study illustrate the difficulty of the recognition task.

In addition, in contrast to our previous work [22], we present in this paper a novel tactile feature based on the high-frequency response of an object being manipulated. The high-frequency response of human receptors has been shown to be relevant in human grasping [2]. In particular, it has been shown to be valuable during transitions of the grasping task, when a grasp is achieved and for detection of slip during motion. We note that exciting the internal contents of a container often elicits a high-frequency response. We propose and show through experiments that this high frequency response signal can be measured and used as a feature to estimate the internal content of objects being manipulated.

### B. Structure of this paper

The remainder of this paper is divided into two parts. In Section II, we present our first approach to estimating the internal state of objects based on a set of six generic features. We present our experimental results and compare them with the performance of humans on the same task. In Section III, we present our second approach based on high-frequency components in the tactile signal. In a second set of experiments, we show that these features can be used to determine the presence of liquid in a container.

## II. APPROACH I: GENERIC TACTILE FEATURES

Our first approach to internal state recognition requires measuring a small set of features that represent internal object properties. We will first describe the set of hardware and sensing requirements to carry out this approach, present details of the features and the machine learning approach and then show experimental results that validate our approach. We will also describe a switching controller that allows us to hold

objects without crushing them. We will also present details of a human study to compare the performance of the robot and humans for the task of recognizing the state of a container using only tactile feedback.

### A. Requirements

We assume a mobile manipulator with a force-sensitive gripper reports at each point in time its position  $p(t) \in \mathbb{R}$  and velocity  $\dot{p}(t) \in \mathbb{R}$  sensed by motor encoders, and the force  $f(t) \in \mathbb{R}$  measured using fingertip sensors. Fingertip sensors typically consist of an array of pressure elements (e.g. Figure 3). In this section, we formulate our approach based on these sensor observations only.

We also assume the existence of a controller that can apply a required force profile. The aim here is that the controller should not damage the objects but still should be able to grasp the object firmly.

### B. Feature extraction

In this work, we concentrate on internal state recognition using two-fingered grasps. Such grasps involve *pinching* an object between two fingers. In our implementation, a two-fingered robotic gripper was used for the experiments (Figure 3) but our approach can be extended to multi-fingered hands as well by using only two fingers to pinch grasp an object. We will henceforth refer to a two-fingered grasp in expanding on our approach while noting that it could be extended to multi-fingered hands as well. Details of our particular implementation using a two-fingered gripper can be found in a subsequent section (Section II-E) along with a description of the particular hardware we used in our experiments.

In preliminary studies, we found that the position, velocity and force profile for a prototypical grasp executed by two fingers has a shape schematically depicted in Fig. 2. The distance  $p(t)$  represents the distance between the two fingers. It decreases until contact with the object is made. The object may deform slightly but ultimately will result in a steady state where the distance between two fingers stays constant.  $\dot{p}(t)$  corresponds to the velocity of the fingers. The spike indicates the onset of contact.  $f(t)$  represents the total force measured at the fingertips using the tactile sensors. Before contact is made, this value is zero. After the impact, the force reduces again as the object gets deformed and the fingers decelerate. After a while, the motion of the fingers stops and a steady state is reached.

From these profiles, we identified two important points in time: the moment the gripper makes first contact with the object  $t_{\text{first}}$  and the time  $t_{\text{steady}}$  after which the sensor values have converged to a steady state. In practice, we require for the first contact detection that both fingers are in contact with the object, i.e., that the force measurement of both fingers is above a certain threshold  $F$ .  $t_{\text{steady}}$  denotes the point in time where the gripper comes to rest, i.e., its velocity drops below a certain threshold  $V$ :

$$t_{\text{first}} = \arg \min_t |f(t)| > F \quad (1)$$

$$t_{\text{steady}} = \arg \min_{t > t_{\text{first}}} |\dot{p}(t)| < V. \quad (2)$$

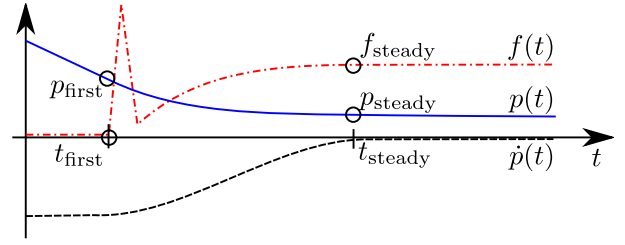


Fig. 2. A schematic drawing of the force/position/velocity profile while grasping an object.

At moment  $t_{\text{first}}$ , we extract the first contact distance  $p_{\text{first}} = p(t_{\text{first}})$ . This is the distance between the two fingertips when contact with the object is first achieved. Note that this is a measure of the uncompressed size of the object. The second feature is the distance between the two fingertips after the gripper has compressed the object fully. We label this the steady state distance

$$p_{\text{steady}} = p(t_{\text{steady}}). \quad (3)$$

Note that this distance is a function of both the material and geometric properties of the object and of the internal state of the object, i.e. whether the object is open or closed and full or empty.

Another useful feature is the time that it takes between making contact with the object and coming to a rest, denoted by

$$\Delta t = t_{\text{steady}} - t_{\text{first}}. \quad (4)$$

Additional features are defined using the force measured by fingertip sensor array. Let  $f_{\text{first}}$  represent the measured force when both the fingertips first make contact with the object. Let  $f_{\text{steady}}$  represent the measured force once the object has stopped compressing. Two other useful features are the average velocity  $\Delta p / \Delta t$  of compression and the average rate of change of the fingertip sensor force  $\Delta f / \Delta t$ , which can be computed from the features from above as follows:

$$\Delta p / \Delta t = (p_{\text{steady}} - p_{\text{first}}) / \Delta t \quad (5)$$

$$\Delta f / \Delta t = (f_{\text{steady}} - f_{\text{first}}) / \Delta t. \quad (6)$$

The average velocity  $\Delta p / \Delta t$  represents the rate at which the object gets compressed and can differ based on the material properties and the geometry of the object. Equivalently,  $\Delta f / \Delta t$  could be thought of as representing an average compression ratio. For computing the measured force, we sum over the measured forces of all cells in the tactile sensor array.

The six generic features summarized in Table I can be easily extracted by most robots equipped with tactile sensors while grasping an object. We do not claim that this list is complete, but by using only this set of features, we were able to reliably estimate the internal state of various containers as described in Section II-E.

### C. Training data

Using the tactile features defined above, we gathered data for a large number of different objects. For each trial, we

Feature	Description
$p_{\text{first}}$	the first contact distance
$p_{\text{steady}}$	distance after which grasping is complete
$f_{\text{steady}}$	force sensed after grasping has completed
$\Delta t$	duration of the grasping
$\Delta p / \Delta t$	average compression velocity
$\Delta f / \Delta t$	average compression ratio

TABLE I

GENERIC SET OF FEATURES THAT CAN BE USED TO CLASSIFY AN OBJECT BEING GRASPED.

obtained measurements for the 6-dimensional feature vector  $\mathbf{a} \in \mathbb{R}^6$ , i.e.,

$$\mathbf{a} = (p_{\text{first}}, p_{\text{steady}}, f_{\text{steady}}, \Delta t, \Delta p / \Delta t, \Delta f / \Delta t)^T, \quad (7)$$

and a label  $c \in C$  describing the object's class and internal state. As a result, we obtained a training database  $\mathcal{D}$  containing a sequence of attribute-class tuples  $(\mathbf{a}, c)$ .

#### D. Decision tree classifier

Subsequently, we have applied a C4.5 decision tree classifier on our training data [23]. We have also tried other supervised classifiers, like support vector machines and neural networks, from which we obtained similar (or slightly worse) results. The reason for this might be that all algorithms are able to extract almost the same amount of data from the training set. The advantage of decision trees over other classifiers is that the learned concepts can intuitively be interpreted. The C4.5 decision tree classifier [24] is an extension of the ID3 algorithm that can deal with continuous attributes.

Decision tree induction is an iterative process: it starts by selecting an attribute that most effectively splits the data according to their data classes. Typically, the information gain (which is the reduction in entropy) is used as a measure for selecting the split. The entropy  $H$  of a set  $\mathcal{D}$  is defined as

$$H(\mathcal{D}) = - \sum_{c \in C} p(c) \log p(c), \quad (8)$$

where  $p(c)$  is the prior probability of target class  $c$  that can be estimated from the training set, i.e.,

$$p(c) = \frac{1}{|\mathcal{D}|} \sum_{(\mathbf{a}, c) \in \mathcal{D}} 1. \quad (9)$$

As all our attributes are continuous, a split  $s$  is defined by a split value  $s_{\text{value}}$  for a particular split attribute  $s_{\text{attr}}$ , i.e., the training set  $\mathcal{D}$  is divided into two subsets

$$\mathcal{D}_{\leq} := \{(\mathbf{a}, c) | a_{s_{\text{attr}}} \leq s_{\text{value}}, (\mathbf{a}, c) \in \mathcal{D}\} \quad (10)$$

$$\mathcal{D}_{>} := \{(\mathbf{a}, c) | a_{s_{\text{attr}}} > s_{\text{value}}, (\mathbf{a}, c) \in \mathcal{D}\}. \quad (11)$$

From all possible splits, C4.5 now selects the one with the highest information gain, i.e.,

$$s = \arg \max_{s \in S} IG(\mathcal{D}, s), \quad (12)$$

where the information gain ( $IG$ ) is defined as the reduction in entropy of the resulting sets compared with the initial set:

$$IG(\mathcal{D}, s) := H(\mathcal{D}) - H(\mathcal{D}|s), \quad (13)$$

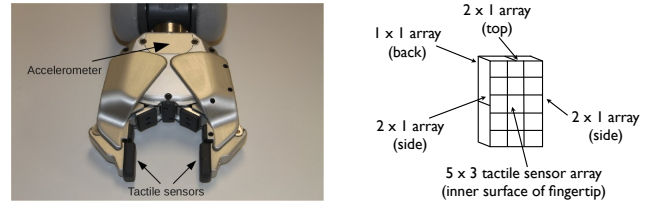


Fig. 3. Left: The PR2 gripper showing the tactile sensors and accelerometer locations. Right: The PR2 has 5x3 tactile sensors on the inside of each finger, 2 sensors on the left, top and right side, and 1 sensor on the back, yielding a total of 22 tactile sensors per finger.

where the conditional entropy  $H(\mathcal{D}|s)$  is defined as

$$H(\mathcal{D}|s) = H(\mathcal{D}_{\leq})p(\leq) + H(\mathcal{D}_{>})p(>). \quad (14)$$

Each split  $s$  corresponds to a node of the decision tree with two children. The same procedure is then repeated for the resulting subsets  $\mathcal{D}_{\leq}$  and  $\mathcal{D}_{>}$ , until the leafs are homogeneous with respect to the target class, i.e., the entropy in the dataset of the leaf is zero.

Another important step after training is pruning, to avoid overfitting to the training data. This is done by replacing a whole subtree by a leaf node if the expected error rate (computed on a test dataset hold out during training) in the subtree is greater than in the single leaf. Due to space constraints, we refer the interested reader to [23] for an excellent introduction to decision tree learning and to [25] for statistical pattern recognition in general.

#### E. Experiments

1) *Hardware*: The hardware used for the experiments in this paper is part of the PR2 robot from Willow Garage. The PR2 is a general-purpose mobile manipulation robot with two arms. Each gripper (see Figure 3) has only a single degree of freedom, actuated by a brushless DC motor with a planetary gearbox and an encoder. The rotary motion of the motor is converted into linear motion of the two fingertips of each gripper. Thus, the PR2 gripper is essentially a parallel jaw single degree of freedom gripper. We used the encoder values for measuring  $p(t)$  and  $\dot{p}(t)$ . The gripper can apply a maximum force of 200 N but is software limited to 100 N. Note that this is also approximately the amount of force that a human can apply by pinching his/her forefinger and thumb together.

Each finger has a capacitive sensor consisting of 22 individual cells mounted on the fingertip. A 5x3 array is mounted on the parallel gripping surface itself while 2 sensors are mounted on the tip of the fingertip, 2 sensors on each side of the fingertip and one on the back, see Figure 3. For this set of experiments, the data from the inner surface of each fingertip was fused into a single measurement  $f_{\text{raw}}(t)$  by summing over all sensor cells. The sensors are capacitive-based pressure sensors and respond to normal pressure exerted on the fingertips. We recorded a calibration curve  $g(f_{\text{raw}}) = f_{\text{calibrated}}$  for the sensors using a load cell. The calibration curve as depicted in Figure 5 was used as a lookup table. As a result, we obtain calibrated values  $f(t) = g(f_{\text{raw}}(t))$  measured in Newtons. Measurements from the tactile sensors on the grippers are obtained at 25 Hz while proprioceptive joint data is measured at 1 KHz. All the



Fig. 4. Some of the bottles and cans used for our experiments. From left to right: Odwalla fruit juice bottle, water bottle, Naked fruit juice bottle, Coke can.

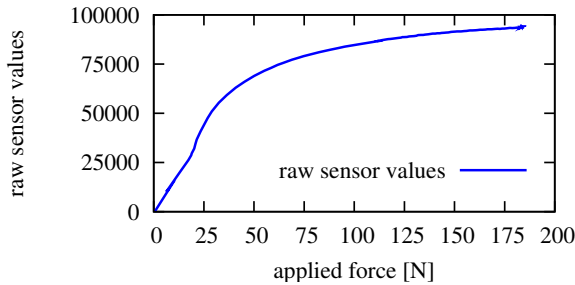


Fig. 5. Calibration data relating raw sensor values to forces calibrated using a load cell.

joints on the robot can be torque controlled using a 1 KHz soft realtime loop. An accelerometer in the gripper measures accelerations in the frame of the gripper. The accelerometer data is sampled at 3 KHz.

2) *Controller*: We explored different controllers for the gripper to achieve the objective of grasping objects without crushing them. A pure velocity controller  $c_{velocity}(\dot{p}(t), t)$  makes the gripper approach an object slowly, but after it contacts the object, it increases its force output in order to establish a constant velocity  $\dot{p}_{target}$ , and thereby crushes the object. Another option is to use a force controller  $c_{force}(f(t), t)$ . Such a controller can hold an object in the hand firmly, by trying to apply a constant force  $f_{target}$ . With a constant force controller, the gripper continuously accelerates until contact is achieved. This can lead to high velocities at impact. As an example, see Figure 6, where the gripper was grasping a very rigid object (here, a wooden block). The significant impact force applied to the object on contact can easily damage rigid, but delicate objects, like eggs. Of course, the applied constant force could be reduced to deal with such cases. In practice, however, if the commanded force is below the force required to overcome static friction, the gripper does not move at all.

Driven by these considerations, we chose to create a switching controller: first, we close the gripper slowly around an object using the velocity controller until it makes contact with the object. Then, we switch seamlessly to the force controller in order to close gently to measure the object’s deformability

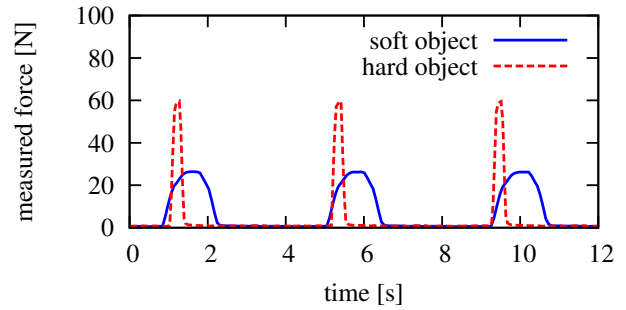


Fig. 6. Measured net fingertip force (N) for grasping a wooden block and a rubber toy when using a pure force controller. The high impact forces can destroy delicate, but rigid objects, like eggs.

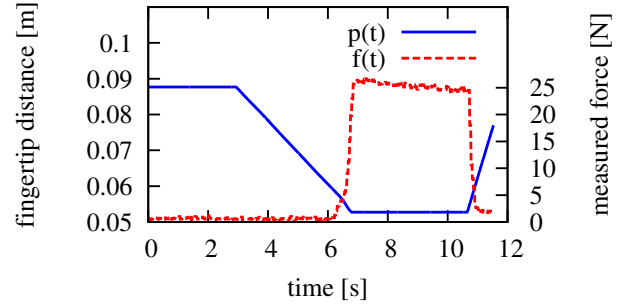


Fig. 7. Fingertip distance and fingertip force vs. time plots showing the reduced impact forces using the hybrid controller. First contact happens at about  $t_{first} = 6$  seconds followed quickly by a steady state at about  $t_{steady} = 6.75$  s where fingertip distance stays constant. The probing effort is set to 23 N. Note that the fingertip force does not spike above the desired probing force on impact.

properties, i.e.,

$$c_{grasping}(t) = \begin{cases} c_{velocity}(\dot{p}(t), t) & \text{while } f(t) = 0 \\ c_{force}(f(t), t) & \text{thereafter.} \end{cases} \quad (15)$$

This hybrid controller has two parameters: both the initial velocity  $\dot{p}_{target}$  and the probing force  $f_{target}$  have influence on the executed grasp.

The result of the hybrid velocity-force controller can be seen in Figure 7. Here, a wooden block was grasped by the gripper using the new controller. The peak force acting on the object is significantly lower. Further, this controller was successful in grasping eggs without crushing them. A movie showing the comparison between an open-loop effort controller and the closed-loop grasping controller is available online<sup>1</sup>.

3) *Experimental setup*: The acquisition of training samples started with the gripper fully open. The containers were placed one at a time between the gripper fingertips, i.e., we did not deal with localizing the object prior to grasping via vision nor moving the gripper towards the object. The gripper was then closed using the hybrid force velocity controller described earlier. Once the gripper came fully to rest, the controller waited for a small interval of time before opening the gripper fully. During each trial, the features described in Sec. II were extracted and written to a file.

The container classes present in the training set are Odwalla fruit juice bottles, Naked fruit juice bottles, soda cans and

<sup>1</sup><http://www.youtube.com/watch?v=fIsMCKOYFEY>

TABLE II

CONFUSION MATRIX FOR RECOGNIZING THE CLASS OF THE CONTAINER, WITH  $f_{\text{TARGET}} = 20\text{ N}$ . THE RECOGNITION RATE IS 93.9%.

a	b	c	d	
58	1	0	1	a = Odwalla fruit juice bottles
8	40	0	0	b = Naked fruit juice bottles
0	0	41	3	c = Softdrink cans
0	0	1	76	d = Water bottles

plastic water bottles, see Figure 4. The internal states of these containers are: closed and full, open and full, open and empty, and closed and empty (except for the soda cans, which cannot be closed again after having been opened). We collected data for each of the internal states for each container class using our switching controller. We carried out a total of 66 trials with 12 Odwalla fruit juice bottles in 4 different internal states, 80 trials with 16 water bottles in 4 different internal states, 42 trials with 12 cans with 3 different internal states, and 41 trials with 10 Naked fruit juice bottles with 4 different internal states. We used different instances of each container class in collecting the data to account for variations within a container class. We also rotated the containers between taking measurements to account for variations in surface properties of individual containers. All this data was collected with the probing force set at 20 N. We also collected a subsequent dataset just for the Odwalla fruit juice bottles using three different probing forces of 17, 20 and 23 N. This involved conducting 24 trials for each internal state for a total of 96 trials for the 4 internal states for each probing force.

To test our classifier we used ten-fold cross validation for each experiment. First, we divided the stratified dataset into 10 parts. Then we learned the classifier on 9 parts, and used it subsequently to classify the test instances from the remaining part. This was repeated for each of the ten folds, such that we ended up with target class predictions for all instances in the dataset. Finally, the predictions were compared to the true target class, and the recognition rate was computed as the ratio between correct and incorrect instances.

#### F. Classification results

The aim for the classification task is to recognize the internal state within each class that indicates whether the container is full or empty and open or closed.

In the first experiment, we found a 93.9% accuracy in recognizing the different liquid containers. Table II shows the confusion matrix for this experiment. From the learned decision trees, this high performance can mainly be attributed to the different size of objects, thus  $p_{\text{first}}$  and  $p_{\text{steady}}$  are very discriminative for this set of containers. Note that our approach is not meant to compete with other senses like vision, but is meant to complement other approaches and to be used for confirmation of a particular object class hypothesis while the robot grasps an object.

After that, we have evaluated the recognition rate of the internal state of a container, given its class. We found that the recognition rate strongly depends on the particular container. This result is not surprising, as obviously feeling the internal state of a container strongly depends on how well it manifests

TABLE III

RECOGNITION RATE, DEPENDING ON THE PROBING FORCE PARAMETER  $f_{\text{TARGET}}$ , FOR THE ODWALLA FRUIT JUICE BOTTLES.

$f_{\text{target}}$	Recognition Rate
17 N	69.8%
20 N	83.3%
23 N	94.8%

TABLE IV

CONFUSION MATRIX OF OUR APPROACH FOR RECOGNIZING THE INTERNAL STATE OF AN ODWALLA FRUIT JUICE BOTTLE FROM THE TACTILE APPEARANCE USING A ROBOTIC GRIPPER ( $f_{\text{TARGET}} = 23\text{ N}$ ). THE RECOGNITION RATE IS 94.8%.

a	b	c	d	
24	0	0	0	a = full closed
0	20	1	3	b = empty open
0	0	24	0	c = full open
1	2	0	21	d = empty closed

its internal state to the outside, i.e., in its tactile appearance. Interestingly, we found that the Odwalla bottles were separable the easiest. Their internal state was estimated correctly at 94.8%, compared to 74.4% for cans, 58.3% for Naked bottles, and only 32.5% for water bottles. The reason for the low performance on water bottles could be that they are made of very flimsy plastic and tend to deform unpredictably.

We also found that the recognition rate was a function of the parameters of our hybrid controller. While the influence of the initial grasping velocity  $\dot{p}_{\text{target}}$  was negligible, we found that choosing a good probing force  $f_{\text{target}}$  could improve the recognition substantially (see Table III). This parameter determines how hard the gripper probes into the object, and should therefore be carefully selected according to the object class. In the case of the Odwalla bottle, we found, for example, the stronger probing force of  $f_{\text{target}} = 23\text{ N}$  to be more informative than weaker ones, yielding a mode recognition rate of 94.8%.

The confusion matrix for the specific case of recognizing the internal state of an Odwalla bottle is shown in Table IV.

In a combined experiment, where we let the robot estimate both the container class and the object internal state except for water bottles (resulting in 11 possible combinations), we obtained a recognition rate of 63.8%.

It is interesting to note that the open and full bottle tends to be compressed for the longest time, i.e.,  $\Delta t$  is large. The steady state force  $f_{\text{steady}}$  differentiates between the open and empty bottle and the empty and closed bottles while the steady state distance  $p_{\text{steady}}$  differentiates the closed and full bottle very easily. However, when we repeated this experiment with bottles that had been subjected to repeated compressions, the recognition rate decreased again to 81%. This is not surprising considering that the classifier was trained on data from fresh bottles while the testing was now done with bottles that had been subject to repeated stress. A movie showing the system recognizing the internal state of a set of bottles using the learned classifier can be found online<sup>2</sup>.

<sup>2</sup><http://www.youtube.com/watch?v=O9i3IcDc5HM>

TABLE V  
OVERALL CONFUSION MATRIX FOR ALL HUMAN SUBJECTS FOR  
RECOGNIZING INTERNAL STATE OF AN ODWALLA FRUIT JUICE BOTTLE.  
THE RECOGNITION RATE IS 75.2%.

a	b	c	d	
48	8	5	0	a = empty open
5	41	1	3	b = empty closed
16	11	55	2	c = full open
2	8	7	63	d = full closed

### G. Comparison with Human Performance

The experimental results show that the robot could do reasonably well in terms of recognizing both the container class in the first series of experiments and internal state of an object in a second series of experiments.

We designed a human study to compare the performance of the robot to that of humans for the internal state estimation problem. The study was designed to find out if, using only tactile feedback, humans could achieve comparable recognition rates for the task of recognizing the internal state of an object. Figure 1 (top right) shows the experimental setup used for the human study. Test subjects were asked to recognize, using only tactile information from squeezing a bottle, the internal state of the bottle. They were provided the opportunity to train beforehand until they were confident about their ability to discriminate between the different internal states of the bottles. Each test subject was then asked to identify the internal state of 16 different bottles sequenced in a random order. The subjects were instructed not to move or pick up the bottles and could not see the bottles while they were grasping them. To simulate the two-fingered grasp used by the gripper, the test subjects were asked to use only their thumb and index finger for the grasping task. Additionally, noise-canceling headphones were used to minimize the sound cues that subjects could pick up. There were a total of 17 test subjects.

Table V shows the overall confusion matrix for all the trials together. The average recognition rates for all the subjects was 75.2%. The highest recognition rate was for bottles that were full and closed. There was considerable confusion between the empty/closed and full/open bottles. Based on a questionnaire filled out by the subjects at the end of the test, we found that most subjects were using features similar to the ones chosen for the learning approach. The two most cited features by the human subjects were the total compression distance and the rate at which the bottle returns to its original shape. The second feature is easier for humans to detect than the robot since the grippers on the robot are not easily back-drivable. The most successful test subjects cited a different set of features to discriminate between the bottles. They used high-frequency feedback from tapping the bottle with their fingers to detect the presence or absence of liquid in the bottle. In the next section, we show how similar information can be used by the robot as well to detect the internal state of containers.

### III. APPROACH II: HIGH FREQUENCY INFORMATION

Several human subjects cited their use of high-frequency feedback from tapping the container with their fingers as critical to the success of their recognition efforts. Gaining such



Fig. 8. Containers used for experiments to determine presence of liquid. Top row (left to right): Sauve, Nesquik, Dry Erase Cleaner, Zero Calorie, 409 containers, Middle row (left to right): tape dispenser, Odwalla Orange, Might Mango, Summer Lime, Green Tea, dummy weight, Bottom row (left to right): Tropicana, water bottle, Coffee Mate, CVS HP and Palmolive containers.

information with a robot, however, requires the ability to excite an object sufficiently fast and the ability to sense the response of the object to such actuation. Most robotic hands do not have the high bandwidth necessary for such actuation. In our case, the gripper by itself is not fast enough to excite the contents of the container in such a manner. However, we found that we could achieve the desired effect by using the entire arm of the PR2. In this section, we expand on the details of actuation and sensing for the PR2 to be able to use high-frequency information to detect the internal state of objects. We present experimental results that shows how this information can prove useful, in particular, in detecting the presence of liquids inside containers.

#### A. Experiments

Figure 1 (bottom row) shows snapshots of the actuation procedure for experiments designed to excite the internal contents of objects. The objects used in the set of experiments are liquid containers. Each container is grasped firmly in the gripper of the PR2 and rolled from side to side at about 0.6 Hz. This motion is designed to excite the internal contents of closed containers. Note that if the object were an open container, its contents would spill out as a result of this motion.

In preliminary experiments, we also tried horizontal movements that would have allowed for open containers. However, we found the PR2 to be too slow to sufficiently excite the contents of the probed containers. This forced the use of the strongest joint on the robot (the joint that rolls the wrist from side to side) to sufficiently excite the contents of the container by forcing the liquid to slosh around under the influence of gravity. The overall approach, however, is (in our belief) more generic and should be executable on any robot that is capable of exciting the internal contents of objects at higher frequencies. In particular, we believe that it is also applicable to open containers with liquid in them if the robot were capable of shaking the container from side to side at a high frequency while maintaining it level.

Experimental results are presented here for 15 different containers. Five trials were carried out for 13 containers with liquid in them. The liquids in the different containers included

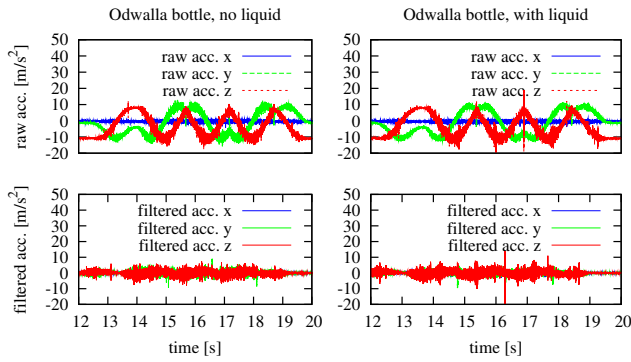


Fig. 9. Accelerometer data corresponding to a container without liquid (left column) and with liquid (right column) for the Odwalla orange juice bottle. The top row shows the raw accelerometer data, the bottom row shows acceleration data filtered using a 5Hz high-pass filter.

water, orange juice, mango juice, shampoo and cleaning fluid, thus representing a good range of viscosity and content. Most of the containers were filled to half their volume with liquid. The *Odwalla Orange* container was tested with two amounts of liquid in it - full and half-full, the *Dry Erase Liquid* container was tested with a full volume of liquid and the *Mighty Mango* and *Sauve* containers were tested when about a quarter full. Five trials each were also carried out for 13 of the containers with no liquid in them, i.e. the contents of the container were completely emptied out. An additional five trials were carried out for a rigid weight that weighed about the same as some of the containers with liquid in them. Figure 8 shows all the containers used in the experiment while Table VII shows statistics for the trials of all containers, including their weights with and without liquid.

### B. Data Analysis

The data measured and recorded for each trial included acceleration data from the accelerometer in the gripper of the robot, tactile sensor data from all 44 elements of the tactile sensors on both fingers of the PR2 gripper and joint positions, velocities and torques for all the moving joints in the arm of the PR2.

Figures 9 and 10 represent two example sets of sensor data for the time period when the container is being rolled: the plots on the left of each figure correspond to data for a container with no liquid in it while the plots on the right correspond to data for a container with liquid in it. The accelerometer data in Figure 9 (top) is noisy and dominated by the component corresponding to the motion of the container. Figure 10 (top) shows the individual tactile sensor responses (for all 44 tactile sensors) over the same period. It is clear that the raw data in this form is not very useful to discern the presence or absence of internal contents in the container.

Our key idea is that liquid sloshing around in a container will produce high-frequency responses that the robot can measure. To that aim, we filtered both the acceleration data and the tactile data, using a high-pass filter on the raw data. After filtering, we condensed the 3- and 44-dimensional signal for the acceleration and tactile data, respectively, into a single, real-valued signal by computing the Euclidean norm of the signal vector.

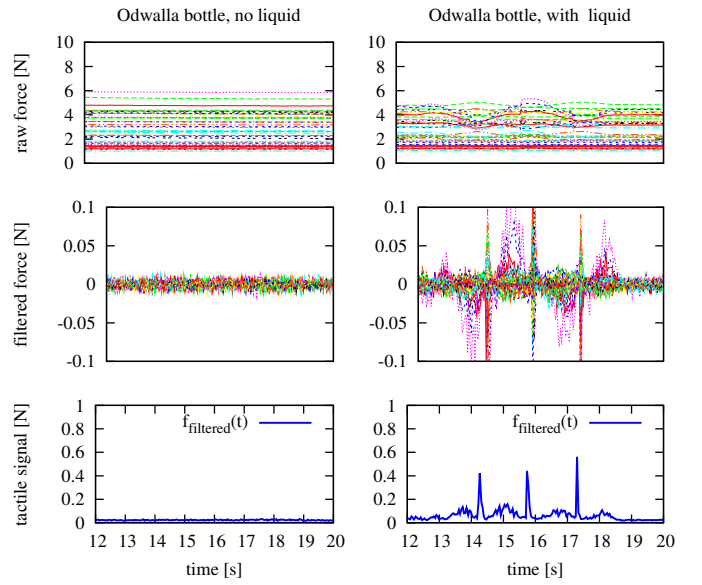


Fig. 10. Tactile sensor data corresponding to a container without liquid (left column) and with liquid (right column) for the Odwalla orange juice bottle. The top row shows the raw tactile pressure measurements of all 44 tactile sensors; the middle row shows these measurements filtered using a 5Hz high-pass filter; the bottom row shows the combined signal of all sensors. The sloshing liquid produces very clear spikes in the bottom right figure.

Figure 9 (bottom row) and 10 (bottom row) show the resulting signal from acceleration data and the tactile sensor data filtered through a 5 Hz high-pass filter, respectively. The filter attenuates the low-frequency components corresponding to the rotation of the container. While the accelerometer signal is slightly different for the two cases, the higher-frequency components in the tactile sensor data, however, are clearly different when the container has liquid in it. The sloshing of the liquid in the container due to its excitation during the rolling of the container results in a spike in the tactile sensor pressure whenever the direction of rotation undergoes a change. This information can easily be computed online and is used to train a classifier that can detect the presence of liquids in containers. For that, we compute the variance in the signal measured by the tactile sensor while the object is being actuated. The difference in this value for the two cases (presence or absence of liquids), is large and consistent across different containers. A summary of our results is given in Table VII.

The accelerometer is significantly affected by the motion of the arm. This makes the acceleration data noisy. It is possible that an accelerometer placed closer to the object (e.g. on the fingertips) may be able to capture better object information. The tactile sensors on the PR2 are closer to the object, and the multiple sensor cells on the sensor can measure the response at multiple points on the object at the same time.

### C. Feature extraction

The high-pass filters we apply to each of the tactile sensors  $i \in 1, \dots, 44$  are first-order Butterworth filters designed with a cutoff frequency of 5 Hz for the sampling rate of 24 Hz. A similar filter (designed for the sampling rate of 3 KHz) is also applied to the accelerometer signal. The use of the 5 Hz cutoff frequency was motivated by experiments that showed

TABLE VI

CONFUSION MATRIX FOR THE ROBOT RECOGNIZING THE FILL STATE OF A BOTTLE USING HIGH-FREQUENCY FILTERING ON TACTILE DATA. THE RECOGNITION RATE IS 91.9%.

a	b	
58	3	a = no liquid
8	67	b = with liquid

that humans possess tactile receptors that specifically react to signals in the 5-50 Hz range when responding to force disturbances [2]. Let  $f_{\text{filtered}}^i$  denote the filtered signal for each individual tactile sensor element (here  $i \in 1, \dots, 44$ ). We combine the signals of all tactile sensor elements into a single signal by computing the Euclidean norm of the filtered signal vectors, i.e.,

$$f_{\text{filtered}}(t) = \left( \sum_{i \in 1, \dots, 44} (f_{\text{filtered}}^i)^2 \right)^{1/2}. \quad (16)$$

From this combined signal, we estimate the sample mean and variance of this signal as

$$\mu = \frac{1}{n} \sum_{t=1, \dots, n} f_{\text{filtered}}(t) \quad \text{and} \quad (17)$$

$$\sigma^2 = \frac{1}{n-1} \sum_{t=1, \dots, n} (f_{\text{filtered}}(t) - \mu)^2, \quad (18)$$

where  $n$  is the number of data samples while the robot was rolling the object and  $t$  refers to the corresponding time indices. In total, we collected data from 136 trials of 15 different containers, see Table VII.

#### D. Decision tree classifier

For detecting the presence of liquid, we use the estimated signal noise  $\sigma$  as the only tactile feature. The target attribute is binary, i.e., either indicating an empty or a filled container. We train a decision tree classifier, as described in Section II-D using ten-fold cross validation. The learned classifier was able to predict the correct internal state of a bottle correctly in 91.9% of the cases. Table VI gives the confusion matrix for this experiment.

By looking at the instances for which prediction errors occurred, we found that all five examples of a full CVS HP bottle were incorrectly classified as empty. This bottle is much smaller than the other containers. As a result, the tactile response is relatively small, when compared with the response of heavier containers.

To remedy this problem, we provided in another experiment the weight of the object in the gripper as a second (additional) feature. By using both the weight and the signal noise, we found a 98.5% correct classification rate. It is important to note here, that the heavy weighted dummy object was classified correctly as containing no liquid, while the light CVS HP bottle was correctly classified as containing liquid. When looking at the learned decision tree, we found that the resulting classifier uses both the tactile signal and weight for predicting the fill state of a container.

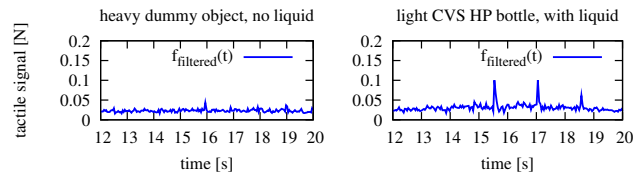


Fig. 11. The heavy dummy object induces virtually no high-frequency component in the signal, while the much lighter CVS HP bottle displays a weak, but clear signal. This shows that our approach does not rely on weight.

#### E. Discussion

In our experimental setup, one might argue that the weight is a strong indicator of the internal state of an object. While it may have some contribution to the observed high-frequency part of the tactile signal induced by the robot's motors, it is worth noting that the corresponding signal shown in Figure 11 for the dummy weight displays virtually no high-frequency component, while the signal of the much lighter CVS HP bottle displays a weak but clear signal. This implies that the presence of liquid in the containers plays a significant role for the observed tactile feature  $f_{\text{filtered}}(t)$ , but that its magnitude depends on the weight of the liquid content.

However, it should be noted that the tactile signal corresponding to a *slip* of the object also has a high-frequency component. Heavier objects are most likely to slip, especially if they are hard to grasp in the parallel jaw gripper of the PR2. A heavier weight (the tape dispenser in Figure 8 weighing about 0.5 kg) does display the same frequency response as containers with liquid in them as shown in Figure 11. The ability to detect shearing forces on the fingertips (using a slip sensor) might allow us to separate out the slip component of the signal, but currently, in the absence of such data, our approach is unable to distinguish between the slip of heavy objects that are grasped awkwardly and containers with liquid in them. A stronger gripper that can grasp heavier objects more firmly would also do well in reducing slip. The other possible modification to our approach which may help to reduce the effect of weight is actuating the containers from side to side while keeping them level.

There are many factors that play a role in the strength of the response for different containers. Smaller containers with smaller amounts of liquid in them (e.g. the CVS HP container) do not display the same strength of response as the bigger containers. Similarly a thick container may damp out the signal before it reaches the tactile sensors. The shape of the containers may also play a part by restricting the ability of the liquid to slosh around inside. Note that one could also use tactile sensors to estimate the weight of the grasped object, and then estimate the content if the weight of the container is known. In contrast to this, we are directly estimating whether something in the container moves in response to the rolling movement. Our approach is therefore more general: a robot using it does not need to know the empty weight of the container. However, knowing additionally the weight of the currently probed container helps the robot to more accurately estimate its internal state.

Object	State	Weight [kg]	Trials	Avg. Tactile Feature [N]
Dummy object	no liquid	0.199	5	0.000 ± 0.000
409	no liquid	0.074	5	0.004 ± 0.001
409	with liquid	0.459	5	0.177 ± 0.104
Coffee Mate	no liquid	0.0417	5	0.003 ± 0.002
Coffee Mate	with liquid	0.3188	5	0.292 ± 0.333
CSV HP	no liquid	0.0268	5	0.001 ± 0.002
CSV HP	with liquid	0.160	5	0.002 ± 0.001
Dry Erase Cleaner	with liquid	0.254	5	0.025 ± 0.014
Green Tea	no liquid	0.033	5	0.000 ± 0.000
Green Tea	with liquid	0.300	5	0.012 ± 0.007
Mighty Mango	no liquid	0.0381	3	0.000 ± 0.000
Mighty Mango	with liquid	0.075	5	0.042 ± 0.026
Nesquik	no liquid	0.038	5	0.000 ± 0.000
Nesquik	with liquid	0.311	5	0.042 ± 0.016
Odwalla Orange	no liquid	0.031	5	0.000 ± 0.000
Odwalla Orange	half full	0.311	5	0.011 ± 0.009
Odwalla Orange	full	0.487	5	0.041 ± 0.018
Palmolive	no liquid	0.045	5	0.000 ± 0.000
Palmolive	with liquid	0.390	5	0.312 ± 0.061
Sauve	with liquid	0.206	5	0.030 ± 0.010
Summer Lime	no liquid	0.029	3	0.008 ± 0.007
Summer Lime	with liquid	0.315	5	0.093 ± 0.043
Tropicana	no liquid	0.032	5	0.000 ± 0.000
Tropicana	with liquid	0.256	5	0.052 ± 0.048
Water Bottle	no liquid	0.014	5	0.000 ± 0.000
Water Bottle	with liquid	0.253	5	0.179 ± 0.035
Zero Calorie	no liquid	0.042	5	0.000 ± 0.000
Zero Calorie	with liquid	0.323	5	0.041 ± 0.022

TABLE VII

USED CONTAINERS IN OUR EXPERIMENTS. THE TACTILE FEATURE IS INDUCED BY LIQUID SLOSHING AROUND IN THE BOTTLE. SMALL BOTTLES WITH LIQUID (LIKE THE CVS HP BOTTLE) YIELD SMALLER VALUES, YET WE ARE NOT MEASURING WEIGHT: THE HEAVY DUMMY OBJECT SHOWS NO RESPONSE AT ALL.

#### IV. CONCLUSION

In this paper, we have presented an approach for estimating the internal state of objects being grasped by a mobile manipulator using tactile sensors. We proposed a set of simple features that can be easily extracted from tactile sensing and proprioception. In experiments carried out on real data, we have shown that both the object class as well as its internal state can be estimated robustly. In a direct comparison experiment, we have shown that the robot's performance is of the same magnitude as human performance. We have also shown the utility of higher-frequency information in detecting the presence of liquids in certain types of containers. From our experiments, we conclude that tactile sensors can be very informative, and can provide valuable information to a mobile manipulation robot.

#### V. ACKNOWLEDGMENTS

The authors acknowledge Joseph Romano for help with setting up the experiments and discussions on the use of high-frequency information. The authors also gratefully acknowledge contributions from the PR2 and ROS development teams in Willow Garage. This work has been partly supported by the EC within the 7th Framework Programme under grant agreement no FP7-248258-First-MM.

#### REFERENCES

- [1] R. S. Johansson, "Sensory and memory information in the control of dexterous manipulation," *Neural Bases of Motor Behaviour*, pp. 205–260, 1996.
- [2] R. S. Johansson and J. R. Flanagan, "Coding and use of tactile signals from the fingertips in object manipulation tasks," *Nature Reviews Neuroscience*, vol. 10, pp. 345–359, May 2009.
- [3] I. Birznieks, V. G. Macefield, G. Westling, and R. S. Johansson, "Slowly adapting mechanoreceptors in the borders of the human fingernail encode fingertip forces," *J. Neurosci.*, vol. 29, no. 29, pp. 9370–9379, 2009.
- [4] R. Dahiya, G. Metta, M. Valle, and G. Sandini, "Tactile sensing: From humans to humanoids," *IEEE Transactions on Robotics*, vol. 26, no. 1, pp. 1–20, 2010.
- [5] J. Tegin and J. Wikander, "Tactile sensing in intelligent robotic manipulation - a review," *Industrial Robot: An International Journal*, vol. 32, no. 1, pp. 64–70, 2005.
- [6] K. Weiss and H. Wörn, "The working principle of resistive tactile sensor cells," *Proc. of the IEEE Int. Conf. on Mechatronics & Automation*, 2005.
- [7] Y. Ohmura, Y. Kuniyoshi, and A. Nagakubo, "Conformable and scalable tactile sensor skin for curved surfaces," in *Proc. of the IEEE Int. Conf. on Robotics & Automation (ICRA)*, Orlando, Florida, USA, 2006, pp. 1348–1353.
- [8] J. Ueda, Y. Ishida, M. Kondo, and T. Ogasawara, "Development of the naist-hand with vision-based tactile fingertip sensor," in *Proc. of the IEEE Int. Conf. on Robotics & Automation (ICRA)*, Barcelona, Spain, 2005, pp. 2332 – 2337.
- [9] K. Motoo, T. Fukuda, F. Arai, and T. Matsuno, "Piezoelectric vibration-type tactile sensor with wide measurement range using elasticity and viscosity change," *Journal of the Robotics Society of Japan*, vol. 24, no. 3, pp. 408–415, 2006.
- [10] C. Williams, D. Shang, and H. Carnahan, "Pressure is a viable controlled output of motor programming for object manipulation tasks," in *Haptics: Generating and Perceiving Tangible Sensations*, ser. Lecture Notes in Computer Science, A. Kappers, J. van Erp, W. Bergmann Tiest, and F. van der Helm, Eds. Springer Berlin / Heidelberg, 2010, vol. 6192, pp. 339–344.
- [11] J. Monzee, Y. Lamarre, and A. Smith, "The effects of digital anesthesia on force control using a precision grip," *Journal of Physiology*, vol. 89, no. 2, pp. 672–683, 2003.
- [12] W. McMahan, J. Romano, A. Abdul Rahuman, and K. Kuchenbecker, "High frequency acceleration feedback significantly increases the realism of haptically rendered textured surfaces," in *Proc. of the IEEE Haptics Symposium*, 2010, pp. 141–148.
- [13] A. Bierbaum, M. Rambow, T. Asfour, and R. Dillmann, "Grasp affordances from multi-fingered tactile exploration using dynamic potential fields," Paris, France, 2009, pp. 168–174.
- [14] A. Schneider, J. Sturm, C. Stachniss, M. Reiser, H. Burkhardt, and W. Burgard, "Object identification with tactile sensors using bag-of-features," in *Proc. of the IEEE/RSJ Int. Conf. on Intelligent Robots and Systems (IROS)*, 2009.
- [15] N. Gorges, S. Navarro, D. Göger, and H. Wörn, "Haptic object recognition using passive joints and haptic key features," in *Proc. of the IEEE Int. Conf. on Robotics & Automation (ICRA)*, Anchorage, Alaska, USA, 2010, pp. 2349–2355.
- [16] S. Takamuku, A. Fukuda, and K. Hosoda, "Repetitive grasping with anthropomorphic skin-covered hand enables robust haptic recognition," in *Proc. of the IEEE/RSJ Int. Conf. on Intelligent Robots and Systems (IROS)*, Nice, France, 2008, pp. 3212–3217.
- [17] J. Sinapov, M. Wiemer, and A. Stoytchev, "Interactive learning of the acoustic properties of household objects," in *Proc. of the IEEE International Conference on Robotics & Automation (ICRA)*, Kobe, Japan, 2009.
- [18] T. Maeno, "Friction estimation by pressing an elastic finger-shaped sensor against a surface," *IEEE Transactions on Robotics and Automation*, vol. 20, no. 2, pp. 222–228, 2004.
- [19] R. Matuk Herrera, "Multilayer perceptrons for bio-inspired friction estimation," in *Proc. of the Int. Conf. on Artificial Intelligence and Soft Computing (ICAISC)*, 2008, pp. 828–838.
- [20] B. Frank, R. Schmedding, C. Stachniss, M. Teschner, and W. Burgard, "Learning the elasticity parameters of deformable objects with a manipulation robot," in *Proc. of the IEEE/RSJ International Conference on Intelligent Robots and Systems (IROS)*, Taipei, Taiwan, 2010.
- [21] H. Saal, J. Ting, and S. Vijayakumar, "Active estimation of object dynamics parameters with tactile sensors," in *Proc. of the IEEE/RSJ Int. Conf. on Intelligent Robots and Systems (IROS)*, Taipei, Taiwan.

- [22] S. Chitta, M. Piccoli, and J. Sturm, "Tactile object class and internal state recognition for mobile manipulation," in *Proc. of the IEEE International Conference on Robotics & Automation (ICRA)*, Anchorage, Alaska, 2010. [Online]. Available: <http://www.informatik.uni-freiburg.de/~sturm/media/chitta2010icra.pdf>
- [23] I. Witten and E. Frank, *Data Mining: Practical Machine Learning Tools and Techniques*. Morgan Kaufmann, 2005.
- [24] J. R. Quinlan, "Learning with continuous classes," in *5th Australian Joint Conference on Artificial Intelligence*, Singapore, 1992, pp. 343–348.
- [25] C. M. Bishop, *Pattern Recognition and Machine Learning (Information Science and Statistics)*. Springer, October 2007.



**Sachin Chitta** Sachin Chitta is a research scientist at Willow Garage, Inc. His research interests are in motion planning, control, and sensing for mobile manipulation in unstructured environments. Dr. Chitta received his Ph.D. in Mechanical Engineering from the University of Pennsylvania in 2005, and he was a postdoctoral researcher working on learning for quadruped locomotion and modular robotics in the GRASP Lab at Penn from 2005 to 2007. Dr. Chitta's research at Willow Garage has led to applications for tasks like autonomous door opening, cart pushing,

object retrieval and tactile sensing.



**Jürgen Sturm** Jürgen Sturm is a Ph.D. student in the Autonomous Intelligent Systems group at the Department of Computer Science of the University of Freiburg, Germany since 2007. He visited Willow Garage as a summer intern in 2009. His major research interests lie in learning models of articulated objects, for example for operating furniture in domestic environments using service robots. He has also worked on tactile sensing, body schema bootstrapping, and imitation learning for mobile manipulation. Before 2007, he studied artificial intelligence

at the University of Amsterdam, where he was a member of the Dutch Aibo Team.



**Matthew Piccoli** Matthew Piccoli is a Ph.D. student in the Department of Mechanical Engineering at the University of Pennsylvania where he works in the Modular Robotics lab with Professor Mark Yim. He received his B.S.E. in Mechanical Engineering from the University of Pennsylvania in 2009. His research interests include grasping, quick-release end effectors, UAVs and modular robots. He visited Willow Garage as a summer intern in 2008 and 2009 working on assisted teleoperation, tactile sensing and grasping.



**Wolfram Burgard** Prof. Wolfram Burgard received his Ph.D. in Computer Science from the University of Bonn in 1991. From 1991 to 1999 he was postdoctoral researcher at the Department of Computer Science of the University of Bonn. In 1999, he became professor for Computer Science at the University of Freiburg where he heads the Laboratory for Autonomous Intelligent Systems (AIS). He and his group have published two books and over 250 articles in the overlapping area of robotics and artificial intelligence. He has received eight best

paper awards from major conferences, the Gottfried Wilhelm Leibniz Prize of the German Research Foundation (DFG), and is Fellow of the AAAI and ECCAI. He and his group actively developed navigation systems for autonomous robots that were deployed as tour-guides in museums, explored abandoned mines and controlled autonomous cars.